# A Tapped-Delay-Line Superconductive Chirp Filter in Shielded Microstrip

Roland Ramisch, *Member, IEEE*, Gerhard R. Olbrich, *Member, IEEE*, and Peter Russer, *Senior Member, IEEE*

*Abstract*—**A superconducting chirp filter having a dispersive time delay of 26 ns and a 3.4 GHz bandwidth centered at 4.7 GHz has been fabricated using a niobium-on-silicon shielded microstrip technology. Along a 2×1.6 m delay line, unequally spaced microstrip directional couplers are employed as sampling devices. To achieve an improvement in dispersion and coupler directivity over conventional microstrip, the device uses a superconductive shield mounted at a distance equal to the height of the dielectric on top of the microstrip structure. Structural support of the 70-μm-thin high-resistivity dielectric is provided by a large-area bond to a glass substrate.**

## I. Introduction

THE application of the delay properties of acoustic and electrical transmission lines as the basic element in the synthesis of transfer functions has been known for quite some time [1]. Passive filters making use of such delay, also known as transversal filters, have found applications as matched filters in signal processing devices. The majority of such filters have been constructed using surface-acoustic-wave (SAW) technology to obtain the required delay properties [2]. However, because of the small acoustic wavelengths involved, minimum line widths required by technology as well as propagation losses impose restrictions on the upper frequency limit. Electromagnetic transmission lines with much larger wavelengths offer a way to obtain much higher upper frequency limits.

The most common type of transversal filter is the *chirp filter*, whose pulse response is the time-reversed replica of a chirp signal. Such a device is characterized by a bandpass transfer function and a rising or falling group delay characteristic over frequency, i.e., the complex conjugate of the chirp's spectrum.

The corresponding pulse response yields a signal whose instantaneous frequency, $f_{\text{inst}}$, is a function of time. A linear relationship between increasing or decreasing frequency $f_{\text{inst}}$ and time characterizes a linear *up-* or *down-chirp*, respectively. This corresponds to a linear group delay characteristic over frequency within the passband.

Such a filter using transmission-line sections in the form of coaxial cable and directional couplers as sampling taps was first described in [3]. For chirp filters with time–bandwith products of around 100 and center frequencies of a few GHz, the total delay time required is in the 10–100 ns range. This requires transmission line lengths of several meters. Size reduction to a small volume results in line widths below 100 μm. The use of normal conductors such as copper at these line widths is not feasible as they exhibit too high losses and are therefore limited in bandwidth [4].

The use of superconducting transmission line offers extremely low loss and inherently wide bandwidth owing to its almost purely inductive nature. We have constructed a linear delay versus frequency chirp filter with superconducting niobium lines on high-resistivity silicon with line widths of 45 μm, a total line length of 3.2 m, and a maximum delay time of 26 ns on a substrate area of about 47 mm by 47 mm. To overcome the limitations of conventional microstrip directional couplers we used a superconducting shield closely spaced at a distance equal to the substrate height above the structure.

## II. Design Theory

Applying the principle of stationary phase to chirp signals to approximate the required transfer function [5], [2] yields a group delay $\tau(f)$ that may be taken directly from the relationship of instantaneous frequency, $f_{\text{inst}}$, versus time if $\tau$ is substituted for $t$. The basic block diagram of a tapped-delay-line transversal filter is shown in Fig. 1. The response is constructed by summing contributions obtained through taps of alternating polarity placed along a delay line. Taps are unequally spaced in distance, but at the same phase intervals with respect to the desired time response.

Within a time interval $0 \leqslant t \leqslant T$ that defines the length of the chirp, a linear chirp signal is given by

$$s(t) = S\cos\vartheta(t) \tag{1}$$

with

$$\vartheta(t) = 2\pi f_0\left(t - \frac{T}{2}\right) + \frac{\mu}{2}\left(t - \frac{T}{2}\right)^2 + \vartheta_0 \tag{2}$$

where $f_0$ is the center frequency. If we interpret the chirp as having an instantaneous frequency $f_{\text{inst}} = \frac{d}{dt}\vartheta(t)$ that

Manuscript received November 15, 1990; revised February 19, 1991. This work was supported by Siemens AG and by the Deutsche Forschungsgemeinschaft.

The authors are with the Technische Universität München, Arcisstr. 21, D-8000 München 2, Germany.

IEEE Log Number 9101128.

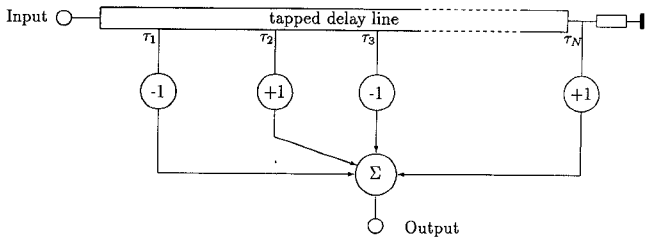


Fig. 1. Block diagram of a transversal filter.

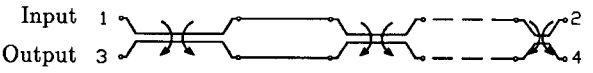


Fig. 2. Two-branch delay line with couplers.

is a linear function of time, then $\mu/2\pi$ is the rate of frequency change.

In order to realize a chirp pulse response utilizing a tapped delay line, the total phase change over time is divided into $N$ intervals of equal size $\Delta\vartheta$ and sampling points are defined to be at the center of each interval. A set of $N$ samples defined by

$$\vartheta_i(\tau_i) = \left(i - \frac{1}{2}\right)\Delta\vartheta, \qquad 1 \leqslant i \leqslant N \tag{3}$$

is obtained. This corresponds to unequally spaced intervals in time. If these intervals are realized by tapping along the line, the delay times, $\tau_i$, are the solutions of $\vartheta(\tau_i) - \vartheta_i(\tau_i) = 0$ with appropriate choice of $\vartheta_0$ such that $\vartheta > 0$. Then $\tau_i$ becomes

$$\tau_i = \frac{1}{\mu}\left[-2\pi f_0 + \sqrt{(2\pi f_0)^2 + 2\mu\left[\left(i - \frac{1}{2}\right)\Delta\vartheta - \vartheta_0\right]}\right] + \frac{T}{2}. \tag{4}$$

If a pulse is applied to the input of the line, the response at the summing node (Fig. 1), assuming no influence of tapping on the forward-traveling pulse along the line, becomes the sum of all individual tap responses. In practice, tapping is achieved by using a number, $n$, of directional couplers inserted into the delay line. With backward-coupling transmission-line couplers, a design symmetric along its length axis with two lines running in parallel is possible (see Fig. 2). Summing is easily achieved through the second line. Each line branch then has to provide half the required delay, $\tau_i$.

The couplers show band-pass responses around odd harmonics of frequencies $f_1 \cdots f_n$ but may also be considered by their time response. Then, they may be regarded as consisting of two taps of opposite polarity separated by a phase difference $\Delta\vartheta$. The total number of taps then becomes $N = 2n$ and the response at the output node is obtained by

$$h(t) = \sum_{i=1}^{2n} (-1)^i \delta(t - \tau_i). \tag{5}$$

Using the relationship between $\delta$ functions,

$$\delta(t - t_i) = \left|\frac{d}{dt} f(t)\right| \delta[f(t)] \tag{6}$$

and applying it to $f(t) = \vartheta(t) - \vartheta_i(\tau_i) = \vartheta(t) - (i - 1/2)\Delta\vartheta$, we may express the pulse response as

$$h(t) = \left|\frac{d}{dt}\vartheta(t)\right| \sum_{i=1}^{2n} (-1)^i \delta\left[\vartheta(t) - \left(i - \frac{1}{2}\right)\Delta\vartheta\right]. \tag{7}$$

Since there is only a limited number, $2n$, of sampling points, we may also limit the series by means of an envelope function $a(t)$ such that in the case of equally weighted pulses

$$a(t) = \begin{cases} 1 & \text{for } 0 < t < T \\ 0 & \text{elsewhere} \end{cases} \tag{8}$$

holds. Rewriting (7) using

$$\sum_{k=-\infty}^{\infty} (-1)^k \delta[y(t) - k\Delta y] = \frac{1}{\Delta y} \sum_{m=-\infty}^{\infty} \exp\left[\frac{j2\pi(2m+1)y(t)}{\Delta y}\right] \tag{9}$$

yields

$$h(t) = a(t)\left|\frac{d}{dt}\vartheta(t)\right| \cdot \frac{1}{\Delta\vartheta} \sum_{m=-\infty}^{+\infty} \exp\left[\frac{j2\pi(m+1)\left(\vartheta(t) + \frac{1}{2}\Delta\vartheta\right)}{\Delta\vartheta}\right]. \tag{10}$$

This is equivalent to a series of cosine waveforms:

$$h(t) = a(t)\left|\frac{d}{dt}\vartheta(t)\right| \frac{2}{\Delta\vartheta} \sum_{p=0}^{+\infty} \cos\frac{(2p+1)\pi\vartheta(t)}{\Delta\vartheta}. \tag{11}$$

If phase intervals are chosen to be spaced 180° apart, i.e.,

$$\Delta\vartheta = \pi \tag{12}$$

the response becomes

$$h(t) = a(t)\left|\frac{d}{dt}\vartheta(t)\right| \frac{2}{\pi} \sum_{p=0}^{+\infty} \cos[(2p+1)\vartheta(t)] \tag{13}$$

or

$$h(t) = a(t)\frac{\left[2\pi f_0 + \mu\left(t - \frac{T}{2}\right)\right]}{\pi} \cdot 2\sum_{p=0}^{+\infty} \cos\left\{(2p+1)\left[2\pi f_0\left(t - \frac{T}{2}\right) + \frac{\mu}{2}\left(t - \frac{T}{2}\right)^2 + \vartheta_0\right]\right\} \tag{14}$$

which, besides an amplitude factor, contains the fundamental chirp waveform ($p = 0$) and its odd harmonics ($p \geqslant 1$). Their harmonic spectra may be calculated by applying the principle of stationary phase [5], and one obtains passband responses centered on odd multiples of $f_0$ with corresponding bandwidths of $(2p+1)B$. The prin-

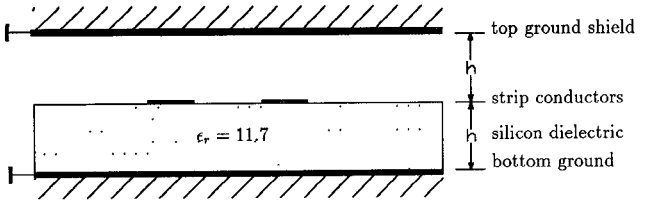


Fig. 3. Shielded microstrip structure on silicon substrate.

ciple of stationary phase states that, in the case of large time–bandwidth products $TB$, the primary contribution to the spectrum of a chirp signal at any frequency point within the passband occurs at and around a time when the instantaneous frequency of the chirp wave passes just that frequency point. This also applies to harmonic spectra centered on odd multiples of $f_0$.

Still, overlapping of the fundamental with the third harmonic may occur if the upper band limit $f_0 + B/2$ of the fundamental falls into a range $3(f_0 \pm B/2)$, i.e., the spectrum of the third harmonic. The condition limiting the possible bandwidth then roughly becomes

$$B < f_0. \tag{15}$$

Any higher harmonics may be suppressed by using a low-pass filter connected at the output of the device. In the above analysis, couplers were considered regarding their time-domain response. This leads to the suppression of even harmonics of the chirp, as would also be expected when considering the band-pass response of couplers at $f_0, 3f_0, 5f_0, \cdots$ in the frequency domain.

A deterioration of the desired response caused by cancellation effects may occur if the couplers show poor directivities. Further, coupling strengths have to be sufficiently low not to weaken the forward-traveling wave along the line substantially. Under this condition ordinary microstrip couplers show poor directivity [6]. Stripline couplers show better performance and have thus been used in superconducting chirp filters [7], [8]. Using line widths measuring around 50 $\mu$m, the substrate thickness has to be reduced to similar dimensions to obtain lines with standard 50 $\Omega$ impedance. If a stripline geometry is used, this imposes a high demand on surface flatness as substrates have to be sandwiched together.

Our design uses a different approach, as shown in Fig. 3. By using a conductive shield spaced at a distance equal to the substrate thickness above the strips, equalization of even- and odd-mode propagation velocities in the couplers is obtained [9]. The effective dielectric constant of the structure in Fig. 3 for even and odd modes is given by [6]

$$\epsilon_{r,\text{eff}} = \frac{\epsilon_r + 1}{2}, \tag{16}$$

Using the above $\epsilon_{r,\text{eff}}$, couplers can then be designed using standard stripline methods. For lines of 50 $\Omega$ characteristic impedance on a 70-$\mu$m-thick high-resistivity silicon substrate of $\epsilon_r = 11.7$, $\epsilon_{r,\text{eff}} = 6.35$ follows, and line widths of about 45 $\mu$m are required. Line spacing in the couplers was chosen to be 100 $\mu$m, giving a coupling strength of $-27$ dB. To avoid unwanted coupling effects in parallel line sections outside of the couplers, lines were spaced 350 $\mu$m apart. This yields coupling strengths of $> 70$ dB.

A straightforward synthesis of the lengths of coupled and uncoupled sections was done on the basis of the linear $\tau(f)$ dependence. Couplers were placed at every $2\pi$ phase interval of the pulse response. Design goals were a maximum time–bandwidth product of 100 and a delay time of about 27 ns with lower and upper chirp frequencies of 3 and 6.6 GHz, respectively. A total of 133 couplers were used in the filter.

Superconductor surface loss resistance was calculated using the Mattis–Bardeen theory [10], [11]. With all conductor layers consisting of 450-nm-thick niobium, the calculated surface loss resistance rises from $3 \cdot 10^{-7}$ $\Omega$ at 1 GHz to $2 \cdot 10^{-5}$ $\Omega$ at 10 GHz and follows an $f^{1.8}$ dependence. Maximum calculated line attenuation caused by conductor losses at 6.6 GHz amounts to $1.2 \cdot 10^{-2}$ dB/m. Since surface roughness effects will be present, higher actual values of conductor attenuation have to be taken into account. Assuming a dielectric loss factor $\tan\delta_\epsilon = 1 \cdot 10^{-5}$ for high-resistivity silicon at 4.2 K [12], the amount of dielectric loss is calculated to a frequency-dependent value of $2 \cdot 10^{-3}$ dB m$^{-1}$ GHz$^{-1}$. At the upper frequency end of the chirp, this yields $1.4 \cdot 10^{-2}$ dB/m.

## III. Circuit Simulation

Starting from initial design data, i.e., bandwidth, center frequency, maximum time delay, and strengths of couplers, line and coupler dimensions were synthesized and used as input data for subsequent circuit analysis. The analysis was carried out in the frequency domain and the filter was divided into individual four-ports as shown in Fig. 4, with each four-port consisting of a coupled-line section. In this way, unwanted coupling effects in delay sections were also taken into account. However, no degrading influence could be noticed when results were compared with calculations with coupling effects in "uncoupled" sections set to zero.

Four-port analysis of coupling sections is possible by dividing couplers along symmetry planes into four half-sections and considering the even- and odd-mode reflection coefficients $r_{e\infty}, r_{e0}, r_{o\infty}, r_{o0}$ for open and short-circuited sections [6]. The scattering matrix $\boldsymbol{S}_i$ of the $i$th coupling section is then given by

$$\boldsymbol{S}_i = \begin{bmatrix} s_{i11} & s_{i12} & s_{i13} & s_{i14} \\ s_{i12} & s_{i11} & s_{i14} & s_{i13} \\ s_{i13} & s_{i14} & s_{i11} & s_{i12} \\ s_{i14} & s_{i13} & s_{i12} & s_{i11} \end{bmatrix} = \begin{bmatrix} \boldsymbol{S}_{i11} & \boldsymbol{S}_{i12} \\ \boldsymbol{S}_{i12} & \boldsymbol{S}_{i11} \end{bmatrix} \tag{17}$$

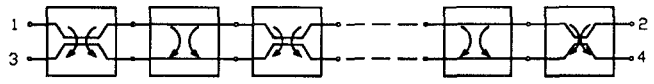


Fig. 4. Division of filter into individual four-ports for simulation.

with

$$s_{i11} = \frac{1}{4}(r_{ie\infty} + r_{ie0} + r_{io\infty} + r_{io0})$$

$$s_{i12} = \frac{1}{4}(r_{ie\infty} - r_{ie0} + r_{io\infty} - r_{io0})$$

$$s_{i13} = \frac{1}{4}(r_{ie\infty} + r_{ie0} - r_{io\infty} - r_{io0})$$

$$s_{i14} = \frac{1}{4}(r_{ie\infty} - r_{ie0} - r_{io\infty} + r_{io0}) \tag{18}$$

where

$$r_{ie\infty} = \frac{1 - j\dfrac{Z_0}{Z_{\text{even}}}\tan\dfrac{1}{2}\theta_i(\omega)}{1 + j\dfrac{Z_0}{Z_{\text{even}}}\tan\dfrac{1}{2}\theta_i(\omega)}$$

$$r_{ie0} = \frac{1 + j\dfrac{Z_0}{Z_{\text{even}}}\cot\dfrac{1}{2}\theta_i(\omega)}{1 - j\dfrac{Z_0}{Z_{\text{even}}}\cot\dfrac{1}{2}\theta_i(\omega)}$$

$$r_{io\infty} = \frac{1 - j\dfrac{Z_0}{Z_{\text{odd}}}\tan\dfrac{1}{2}\theta_i(\omega)}{1 + j\dfrac{Z_0}{Z_{\text{odd}}}\tan\dfrac{1}{2}\theta_i(\omega)}$$

$$r_{io0} = \frac{1 + j\dfrac{Z_0}{Z_{\text{odd}}}\cot\dfrac{1}{2}\theta_i(\omega)}{1 - j\dfrac{Z_0}{Z_{\text{odd}}}\cot\dfrac{1}{2}\theta_i(\omega)}. \tag{19}$$

Because of equal even- and odd-mode phase velocities, the same electrical length $\theta_i(\omega)$ appears in even and odd modes. After transforming individual four-port $S$ parameters into $T$-parameter representations,

$$\boldsymbol{T}_i = \begin{bmatrix} \boldsymbol{S}_{i12} - \boldsymbol{S}_{i11}\boldsymbol{S}_{i12}^{-1}\boldsymbol{S}_{i11} & \boldsymbol{S}_{i11}\boldsymbol{S}_{i12}^{-1} \\ -\boldsymbol{S}_{i12}^{-1}\boldsymbol{S}_{i11} & \boldsymbol{S}_{i12}^{-1} \end{bmatrix} \tag{20}$$

$T$ parameters for the complete circuit are obtained as the product of all individual coupler parameters, $\boldsymbol{T} = \prod_{i=1}^{n}\boldsymbol{T}_i$, and may then be retransformed into $S$ parameters. As propagation losses are very small, they may be taken into account by considering a complex propagation constant $\gamma = \alpha + j\beta$ instead of a purely imaginary propagation constant. The term $j\tan\theta_i(\omega)/2 = j\tan\beta l_i/2$ in (19) is then replaced by the appropriate expression according to

$$j\tan\frac{\beta l_i}{2} \Rightarrow \tanh\frac{\gamma l_i}{2}. \tag{21}$$

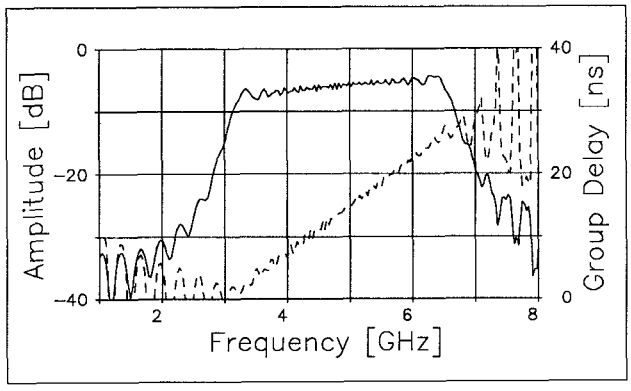


Fig. 5. Simulated transfer characteristic of the chirp filter.

Prior to fabrication, the performance of the filter was simulated assuming 266 coupled sections. Fig. 5 shows the calculated amplitude and delay properties of the filter when operated between ports 1 and 3 with ports 2 and 4 terminated in their characteristic impedances.

## IV. Fabrication

To put the required total line length of two times 1.6 m onto an available substrate area about 50 mm in diameter, the double line was wound in a double spiral as shown in Fig. 6. Lengths of individual sections were calculated as if the lines were laid out along a straight symmetry line. This symmetry line was then wound to double-spiral shape and all coordinates were transformed accordingly. Based on these coordinates, the mask layout was generated. Since coupling between adjacent turns of the spiral should not degrade performance, their spacing was chosen to be 400 $\mu$m, yielding a maximum coupling strength of 86 dB.

Fig. 7 shows a simplified cross-section view of the device. Fabrication starts with a 50.8-mm-diameter wafer of high-resistivity ($>1000\ \Omega\cdot$cm) p-silicon. This specific resistance is large enough that charge carriers freeze out sufficiently when the device is cooled to 4.2 K. A 450-nm-thick superconductive layer of niobium was sputtered onto the high-resistivity surface. This layer later became the bottom ground layer. Using a high-temperature ($\simeq 350°$ C), high-voltage (1 kV) electrostatic bonding technique [13], the whole structure was bonded upside down onto a 50 mm by 50 mm, 1.5-mm-thick carrier of polished Pyrex glass. Because of the elevated temperature, there are enough mobile ions in the glass that react at the glass–niobium interface under the strong electric field that is present there. Fig. 8 shows the two parts prior to bonding. Pyrex was chosen because of its low thermal expansion coefficient—similar to that of silicon, a fact that prevents the bond from breaking when it is cooled to 4.2 K. The technique results in a strong bond, which suffered no damage after many thermal cycles.

Subsequently, the silicon was thinned by polishing it to a thickness of 70 $\mu$m. To get easy access to the line structure for making electrical connections and because

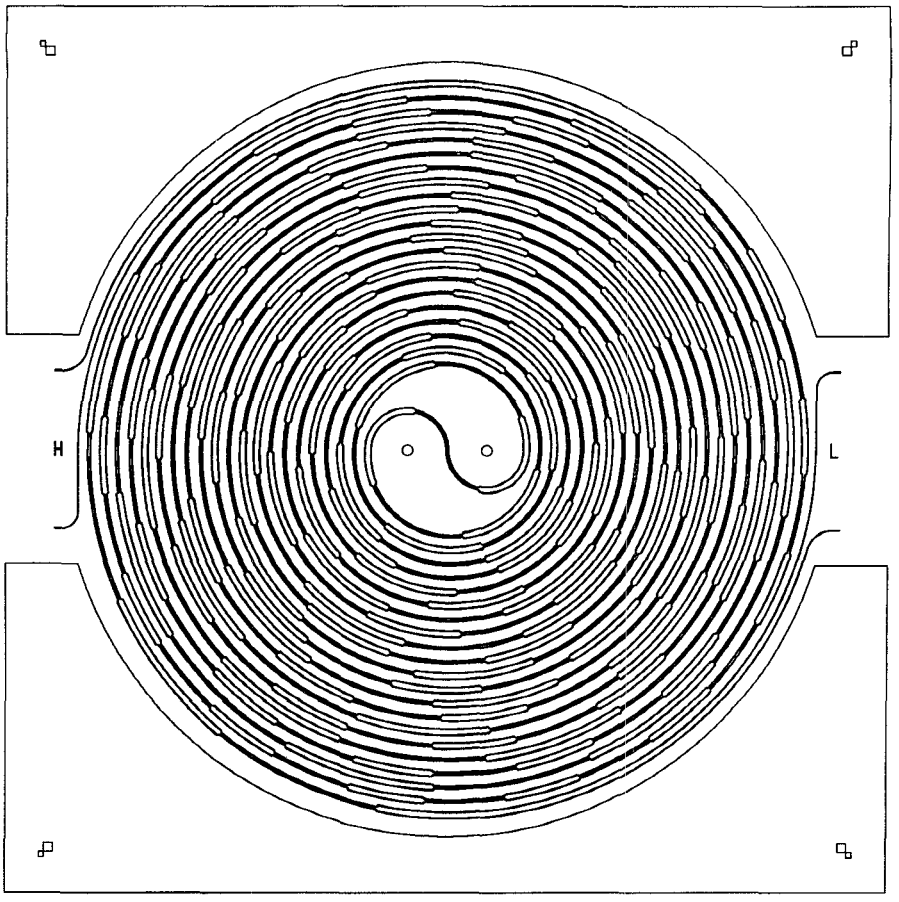


Fig. 6. Conductor layout of the chirp filter.

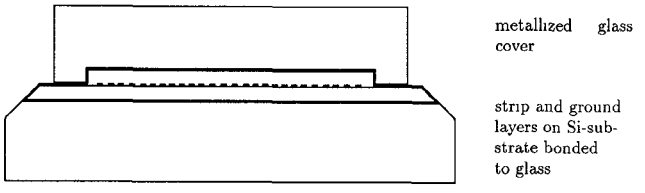


Fig. 7. Simplified cross-sectional view of the device (not to scale).

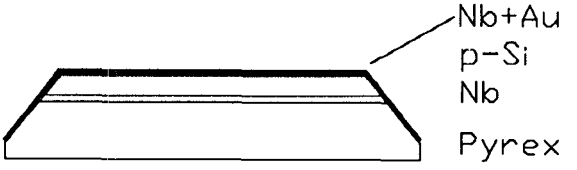


Fig. 9. Cross section of substrate after sputtering (not to scale).

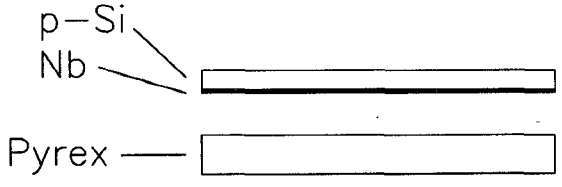


Fig. 8. Pyrex carrier and sputtered silicon before bonding (not to scale).

of size limitations in the opening of the liquid helium Dewar, the whole assembly was reduced to a size of 47 mm by 47 mm by grinding off the edges. By grinding at an oblique angle, access to the ground electrode was obtained.

Now, the Nb layer for the strips plus an additional layer of gold was sputtered onto the top surface (Fig. 9). The gold layer was structured with photoresist and chemical etching, using the mask with the layout obtained as described above. The gold layer was used as an etch mask in the following sputter etch process, which produced the conducting strip. Fig. 6 shows the large-area ground that was formed around the spiral as a contact area to the shield. All gold was removed chemically, except from the large ground area and the contact pads that were used for bonding.

The top cover serves to provide the grounded electric shield at the required distance of 70 $\mu$m above the substrate. It consists of Pyrex glass into which a 70-$\mu$m-deep large-area round hole is etched chemically. On two opposite sides, openings are provided where the conducting strip can be brought out. An etching rate of about 1 $\mu$m per minute was obtained using 26% hydrofluoric acid. Gold was used as an etch mask. After removal of the masking layer, niobium and gold were sputtered onto the etched surface. Inside the 70-$\mu$m-deep hole, gold was removed, so that only the surrounding area retained its gold surface to be used for contacting the bottom ground.

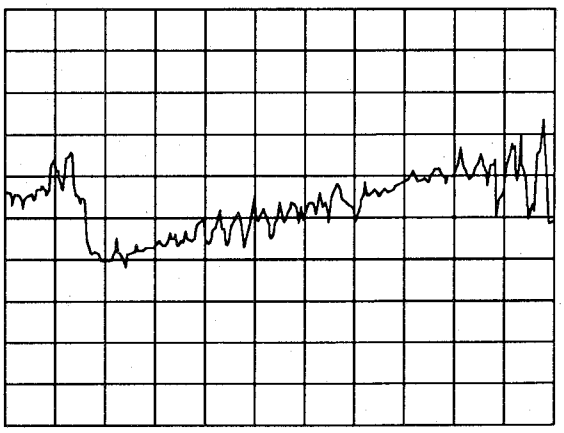

Fig. 10. Measured delay versus frequency characteristic, 2.2–6.8 GHz, 10 ns/div.

The glass-silicon substrate was assembled with the top cover and glued into a brass fixture. The cover was pressed onto the substrate with springs and secured with conductive silver at the rim; this also provided an additional ground connection. Contact to the strip conductors was made by bonding small gold ribbons of 15 $\mu$m thickness directly onto the gold-plated center conductors of semirigid cable. The ends of the semirigid cable were located at the subtrate's rim and secured in the fixture. Where contacts are made, the top cover is recessed, so that the strip, widened to 60 $\mu$m to retain the characteristic impedance, is exposed. Ground contact is made by bonding a large number of gold ribbons from the ground area surrounding the spiral to the fixture.

## V. Device Performance

For device evaluation, connections to the finished device submerged in liquid helium at 4.2 K with 50 $\Omega$ terminations applied at the upper frequency end were made through aluminium semirigid cables because of their low thermal conductivity.

Fig. 10 shows measured group delay versus frequency. A maximum delay time of 26 ns was obtained. Measured loss at the low-frequency end of the chirp was 3 dB greater than calculated. At the upper end of the chirp, measured loss amounted to around 15 dB. The band-pass response of the filter was not as pronounced as expected; however, a fast Fourier transform of the measured response showed the chirp pulse response as predicted. An upper chirp frequency of about 6.4 GHz was obtained, which yields a time–bandwidth product of 88. The reversed delay versus frequency performance when using the high-frequency end of the filter as input and output, as predicted by theory, was also obtained.

Subsequent experiments showed that the performance was influenced mainly by the way ground connections were made, and it was noted that larger-area, less inductive connections to the bottom ground can improve performance. The resistivity of the lower ground plane may have been somewhat degraded by the bonding process, as has been observed by others [14]. However, no further designs that take care of these facts were made so far.

## Acknowledgment

The authors are indebted to Mr. D. Gruchmann of AEG, Ulm, for polishing the substrate.

## References

[1] H. E. Kallman, "Transversal filters," *Proc. IRE*, pp. 302–310, July 1940.
[2] D. P. Morgan, *Surface-Wave Devices for Signal Processing*. Amsterdam: Elsevier, 1985.
[3] F. J. Mueller and R. L. Goodwin, "A wide-band compressive receiver," in *IRE Int. Conv. Rec.*, pt. 3, 1962, pp. 103–119.
[4] R. L. Kautz, "Minituarization of normal-state and superconducting striplines," *J. Res. Nat. Bur. Stand.*, vol. 84, no. 3, pp. 247–259, May–June 1979.
[5] C. E. Cook and M. Bernfeld, *Radar Signals*. New York: Academic Press, 1967.
[6] R. K. Hoffmann, *Handbook of Microwave Integrated Circuits*. Norwood, MA: Artech House, 1987, p. 253. (Translation of *Integrierte Mikrowellenschaltungen*. Berlin: Springer-Verlag, 1983.)
[7] R. S. Withers, A. C. Anderson, P. V. Wright, and S. A. Reible, "Superconductive tapped delay lines for microwave analog signal processing," *IEEE Trans. Magn.*, vol. MAG-19, May 1983.
[8] M. S. DiIorio, R. S. Withers, and A. C. Anderson, "Wide-band superconductive chirp filters," *IEEE Trans. Microwave Theory Tech.*, vol. 37, Apr. 1989.
[9] R. Garg, "Stripline-like microstrip configuration," *Microwave J.*, vol. 4, pp. 103–104, 116, 1979.
[10] D. C. Mattis and J. Bardeen, "Theory of the anomalous skineffect in normal and superconducting metals," *Phys. Rev.*, vol. 111, no. 2, pp. 412–417, 1958.
[11] R. Pöpel, "Auswertung der Mattis-Bardeen-Theorie und Messungen an supraleiten den Mikrostreifenleitungen," thesis, Techn. Universität Braunschweig, Germany, 1986.
[12] M. A. Delaney, "Superconductive delay line with integral MOSFET taps," *IEEE Trans. Magn.*, vol. MAG-23, pp. 791–795, Mar. 1987.
[13] G. Wallis and D. I. Pomerantz, "Field-assisted glass-metal sealing," *J. Appl. Phys.*, vol. 40, no. 10, pp. 3946–3949, Sept. 1969.
[14] R. S. Withers and R. W. Ralston, "Superconductive analog signal processing devices," *Proc. IEEE*, vol. 77, Aug. 1989.

**Roland Ramisch** (S'84–M'89) was born in Kaufbeuren, Bavaria, Germany, in 1956. He obtained the Dipl. Ing. degree in electrical engineering from the Technische Universität München in 1983.

He is currently engaged in analog applications of superconducting circuits at the Lehrstuhl für Hochfrequenztechnik at the Technische Universität München.

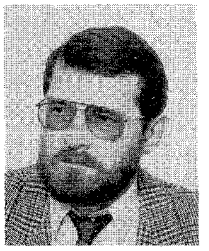

**Gerhard R. Olbrich** (M'86) was born in Neustadt/Waldnaab, Bavaria, Germany, in 1947. He received the Dipl.-Ing. degree in 1974 and the Dr.-Ing. degree in 1979, both in electrical engineering from the Technische Universität München, Germany.

From 1975 to 1985 he was an Assistant Professor at the Institute of Microwave Engineering and the Institute of High Frequency Engineering at the Technische Universität München. During this time he worked on problems of

microwave impedance and frequency measurements and planar hybrid circuits using thin-film technology. From 1986 to 1988 he was president of Work Microwave GmbH, Holzkirchen, Germany, mainly engaged in developing low-phase-noise microwave oscillators. Since 1989 he has again been with the Institute of High Frequency Engineering of the Technische Universität München. His current interests are in the fields of microwave measurement techniques, planar hybrid circuits, and low-phase-noise oscillators.

Dr. Olbrich is a member of the German Informationstechnische Gesellschaft VDE(ITG).

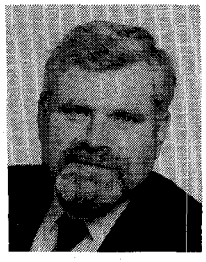

**Peter Russer** (SM'81) was born in Vienna, Austria, in 1943. He received the Dipl. Ing. degree in 1967 and the Dr. techn. degree in 1971, both in electrical engineering and both from the Technische Universität, Vienna, Austria.

From 1968 to 1971, he was an Assistant Professor at the Technische Universität, Vienna. In 1971 he joined the Research Institute of AEG-Telefunken in Ulm, where he worked on fiber-optical communication, high-speed solid-state electronic circuits, laser modulation, and fiber-optic gyroscopes. In 1979 he was a corecipient of the NTG award. Since 1981 he has held the chair of Hochfrequenztechnik at the Technische Universität München, Germany. His current research interests are microwave circuits, electromagnetic fields, statistical noise analysis of microwave circuits, methods for computer-aided design of microwave circuits, integrated microwave and millimeter-wave circuits, microwave oscillators, and microwave applications of superconductors.

Dr. Russer is the author of numerous scientific papers in these fields. He is a member of the German Informationstechnische Gesellschaft and of the Austrian and German Physical Societies. In 1990 he was a Visiting Professor at the University of Ottawa.